Dalton Transactions

Cite this: *Dalton Trans.*, 2012, **41**, 12558

www.rsc.org/dalton

PAPER



# Amidine- and amidinate-functionalised *N*-heterocyclic carbene complexes of silver and chromium†‡

**Susana Conde-Guadano,[a] Martin Hanton,[a] Robert P. Tooze,[a] Andreas A. Danopoulos*[b] and Pierre Braunstein[b]**

***Received 20th July 2012, Accepted 22nd August 2012***
**DOI: 10.1039/c2dt31619f**

A new family of *N*,*N*′-bis-(2,6-diisopropylphenyl)-(2,6-diisopropylphenyl-imidazolium)-acetamidines have been developed as NHC proligands and ligands that are functionalised with neutral amidine and anionic amidinato moieties. On coordination they adopt diverse binding modes, depending on the nature of the metal and the reaction conditions. In the Ag, K and Cr complexes reported in this paper, monodentate $\kappa^1$(NHC), bimetallic bridging-($\kappa^1$-NHC–$\kappa^1$-amidinato) and bidentate ($\kappa^1$-NHC–$\kappa^1$-amidinato) binding modes were observed, respectively. Two of the novel Cr complexes, in the presence of activators, were tested as catalysts for the polymerisation of ethylene showing low activity.

## Introduction

The use of functionalised *N*-heterocyclic carbene (NHC) ligands for the tailoring of the metal coordination sphere appeared very early in the history of development of NHC ligands.[1,2] The demonstration of the versatility, scope and potential of this ligand design concept is now well established and attracting interest from researchers from diverse areas of organometallic, bioinorganic chemistry and catalysis.[3] NHC ligands functionalised with neutral N-donors are particularly attractive, especially with amine,[4] pyridine,[5] imine[6] and other heterocycles. In comparison, fewer examples of NHCs functionalised with anionic N-donors, *i.e.* carboxylic acid amides[7] and dialkylamides,[8–10] have also been studied, the latter mainly on electropositive metals.

The usefulness of amidine and amidinato donors has been amply demonstrated in coordination chemistry, in particular with electropositive metals, where the amidinato as an anionic ligand is usually coordinating in a $\kappa^2$ chelating bidentate mode acting as a 6e$^-$ donor[11] and in catalysis applications.[12,13] Diverse and rich coordination chemistry of the amidinato ligand has been observed that is dependent on the steric and electronic properties of the metal coligands and the amidine moiety substituents.[14] In contrast, neutral amidines preferentially coordinate from the more basic and sterically accessible imine N atom.[15,16]

The versatility of the amidine ligands has further been expanded thanks to their tuning scope by relatively straightforward and adaptable synthetic methods and the additional functionalisation of the amidine core by the attachment of pendant arms bearing classical donor groups at the amine terminus (A in Scheme 1) such as ω-dialkylamino-alkyl-, β-hydroxyalkyl-, β-(2-pyridyl)-ethyl-, 2-lutidinyl-, ferrocenyl-.[17–22]

Less frequently and relatively recently pendant groups have been attached to the amidine and amidinato functionality at the C atom of the amidine using a flexible linker (this excludes guanidines and phosphaguanidines) as shown in B, Scheme 1. Known examples of $L^2$ donors include 2-pyridyl-,[23] 2-furyl-,[24] carboranyl-,[25] and phenoxy-[26] groups, giving rise to tridentate or 'heteroscorpionate' ligand architectures,[27] with potential dynamic behaviour, hemilability and denticity changes. These new ligands are intensely studied in catalytic applications involving electropositive metals.

Amidine and amidinato functionalised NHC ligands and complexes have not been described, albeit they are expected to exhibit high potential for the tuning of the metal coordination sphere. In principle, functionalisation *via* the N-terminus or the C atom of the amidine is conceivable (Scheme 2) leading to a range of coordination modes depending on the length of the

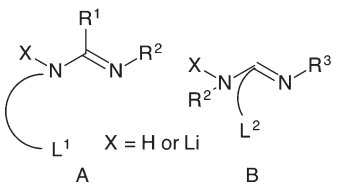


**Scheme 1** Schematic representation of the functionalisation of the amidine moiety by pendant arms attached to the N-terminal atom or the amidine C atom; $R^1$–$R^3$ are alkyl or aryl groups, $L^1$ is amine, pyridine *etc.*, $L^2$ is bis-(pyrazolyl)methyl, phenoxide *etc.* Only one of the possible isomers is shown in each case.

[a]*Sasol Technology UK Ltd, Purdie Building, North Haugh, St Andrews, Fife, UK, KY16 9ST*
[b]*Laboratoire de Chimie de Coordination, Institut de Chimie (UMR 7177 CNRS) Université de Strasbourg, 4 rue Blaise Pascal, F-67081 Strasbourg, France*

† This manuscript is dedicated to the outstanding chemist, colleague and supportive friend Professor David Cole-Hamilton on the occasion of his retirement and for his outstanding contribution to transition metal catalysis.

‡ CCDC 892658–892663. For crystallographic data in CIF or other electronic format see DOI: 10.1039/c2dt31619f

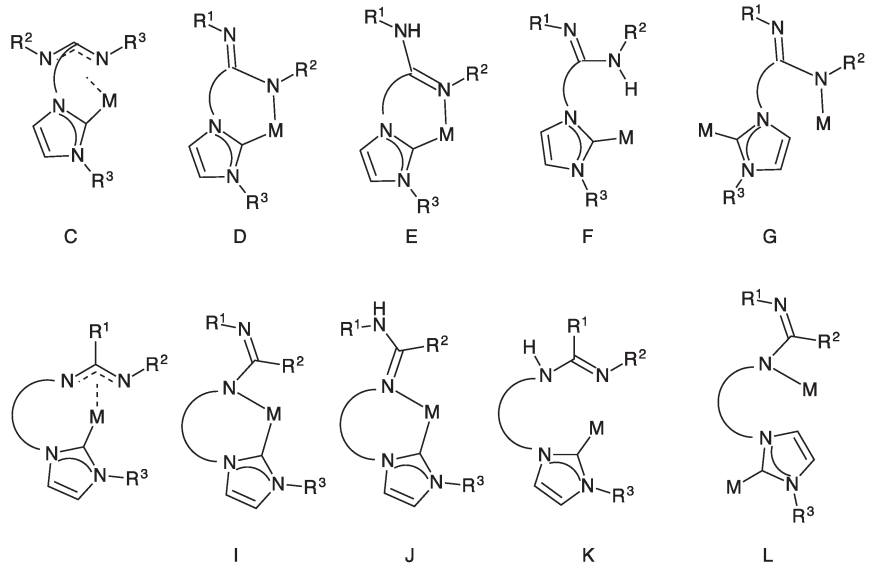


**Scheme 2** Plausible coordination modes of (i) an anionic ligand with the amidinato moiety and NHC donors tethered from the amidine C atom (C and D) or N atom (H, I); (ii) a neutral ligand with one amidine moiety and an NHC donor tethered from the amidine C atom (E) or N atom (J); (iii) a neutral ligand with NHC coordination and the dangling amidine moiety (F and K); and (iv) an anionic ligand with amidinato and NHC donors bridging two metals (G and L). The complexes described here display modes D, E, F and G. Different geometrical and conformational isomers are not depicted.

linker, the bulk of the substituents $R^1$–$R^3$, the nature and oxidation state of the metal and the metallation reaction conditions (kinetic control).

Herein we report the first examples of pro-ligands and ligands in which the imidazolium or the corresponding NHC groups are tethered to the C atom of the amidine *via* a methylene linker. We also describe their K, Ag and Cr complexes which illustrate the scope, diversity and potential of the ligand design. Complexes with other early and late transition metals as well as N-tethered NHC ligand designs will be the subject of forthcoming papers. Preliminary catalytic testing of two Cr complexes in the oligomerisation/polymerisation of ethylene is also reported.

## Results and discussion

### The synthesis of the amidine proligands

The synthetic approach for the proligand $(H_2L)^+Cl^-$ (**4**) and ligands (HL) (**5**) and $(K^+L^-)$ (**6**) used in this work is depicted in Scheme 3.

The chloroacetamidines were obtained from the chloroacetamide **1** with $PCl_5$ in two steps by a modification of the Wolmershäuser methodology,[28] consisting of isolation of the imidoyl chloride **2** by vacuum distillation and subsequent reaction with aniline to the amidine **3**. Quaternisation of the (2,6-$Pr^{ii}_2C_6H_3$)-imidazole by the chloroacetamidine **3** took place only under forcing conditions. Interestingly, self-quaternisation of **3** was not a competing reaction, possibly due to steric reasons.

The appearance of the $^1$H-NMR spectra of **4** in $CDCl_3$ was complex, showing clearly the presence of two main isomers in an approximately 2/3 ratio. This isomeric mixture probably arises from the presence of the *Z* and *E* and *syn* and *anti* isomers in solution (Scheme 4).[29]

The existence of isomers and the corresponding tautomers is common in amidine chemistry and their rate of interconversion (by inversion at the N, rotation around the C=N bond and/or tautomerisation) is dependent on the nature of the amidine substituents and the reaction medium.[28,29] We were not able to carry out full assignment of the $^1$H-NMR spectra. However, support of the presence of two isomers in $CDCl_3$ was provided by the two peaks in the imidazolium proton region as well as for the methylene protons of the linker. Finally, the isopropyl substituents of the diisopropylphenyl rings were non-equivalent and gave three septets and six doublets for *each* isomer. The $^1$H-NMR and $^{13}C\{^1H\}$-NMR spectra in $d_6$-DMSO were much simpler, with the peaks corresponding to the *Z* and *E* isomers converging to one average signal. Therefore the higher polarity of DMSO may favor the interconversion between *Z* and *E* isomers in solution possibly by increasing the rate of tautomerisation. The presence of H-bonding interactions in solution is also possible.

Additional insight into the structure of the imidazolium chloride **4** in the solid state was gained by a single crystal X-ray diffraction study of crystals obtained from chloroform; a representation of the cation in **4** is given in Fig. 1.

The cation that crystallised was the *E-anti* isomer. All bond lengths in the structure of **4** were unremarkable. There are short contacts between the imidazolium proton as well as the amidine proton and the chloride anion (2.56 and 2.45 Å, respectively). There are also close contacts of the chloride anion with one of the backbone hydrogens of the imidazolium ring (2.77 Å) and of the chloroform (2.37 Å).

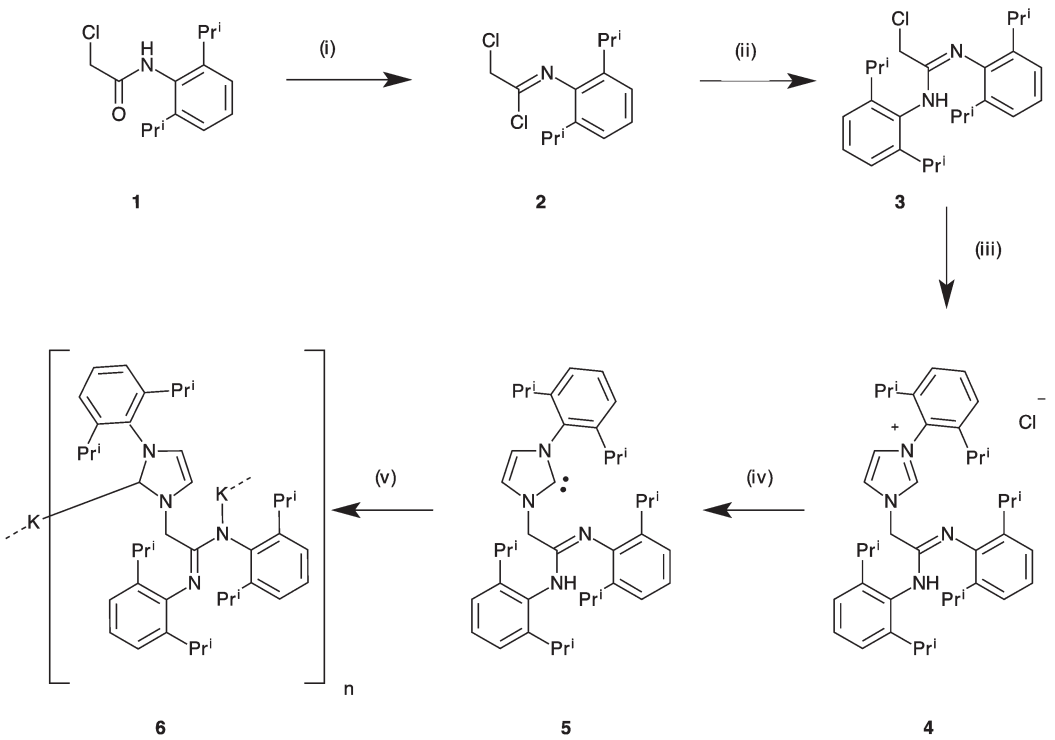


**Scheme 3** Synthetic transformations for the proligands and ligands. Reagents and conditions: (i) 1 equiv. $PCl_5$, $C_6H_6$; (ii) 1 equiv. 2,6-$Pr^i_2C_6H_3NH_2$, RT; (iii) (2,6-$Pr^i_2C_6H_3$)-imidazol; (iv) 1 equiv. $KN(SiMe_3)_2$, $C_6H_6$; (v) $KN(SiMe_3)_2$, $C_6H_6$.

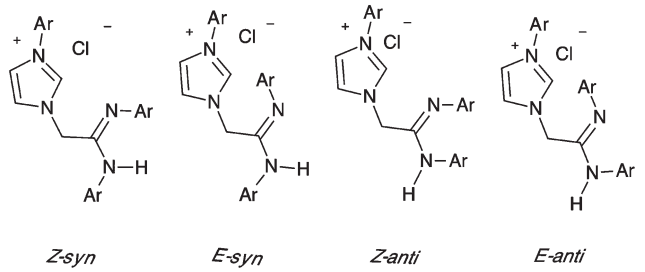


**Scheme 4** Possible geometrical and conformational isomers of the imidazolium salt **4**.

### The synthesis of the neutral NHC amidine and the anionic NHC amidinato potassium ligands

The reaction of the imidazolium chloride **4** with 1 equiv. of $KN(SiMe_3)_2$ in benzene gave the neutral NHC ligand **5** which was isolated as a light yellow air and moisture sensitive powder and was characterised by spectroscopic techniques. The $^1$H- and $^{13}C\{^1H\}$-NMR spectra in $d_6$-benzene gave unequivocal evidence that the first deprotonation occurred specifically at the C–H acidic site rather than the amidine. This was inferred by the disappearance of the imidazolium proton signals at *ca.* $\delta$ 10.95, the persistence of the signals assignable to the amidine protons at $\delta$ 8.05 and the appearance of a signal at $\delta$ 217.0 in the $^{13}C\{^1H\}$ spectrum assignable to the NHC carbon. Generally, the $^1$H-NMR spectrum of **5** showed rather broad signals and was considerably simpler compared to the spectrum of **4** in $CDCl_3$ described earlier. This is certainly due to a faster interconversion between the *Z*- and *E*-isomers in solution although the cause and the mechanism of this process have not been further explored.

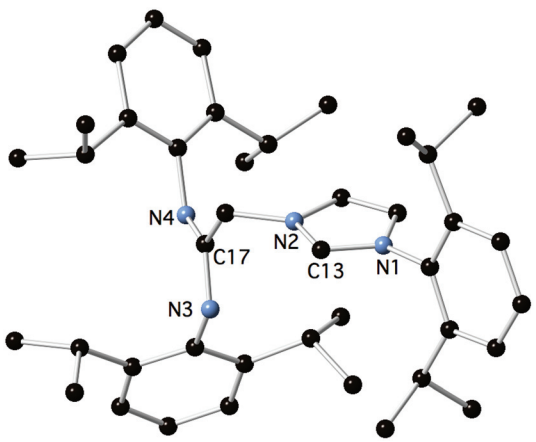


**Fig. 1** Ball-and-stick representation of the structure of the cation in **4**. Solvent molecules ($CHCl_3$) in the asymmetric unit are omitted for clarity. Selected bond lengths (Å) and angles (°): C17–N4 = 1.273(5), C13–N1 = 1.322(5), C13–N2 = 1.334(5), N4–C17–C16 = 125.1(3), N4–C17–N3 = 121.4(3), N3–C17–C16 = 113.4(3), N1–C13–N2 = 108.6(3).

Deprotonation of **5** with a second equivalent of $KN(SiMe_3)_2$ in benzene gave the potassium salt **6** in good yield as an extremely air and moisture sensitive white solid. It was characterised by analytical and spectroscopic methods. The $^1$H-NMR spectrum of **6** in $d_5$-pyridine showed relatively broad features. However, the signals corresponding to the isopropyl substituents of the NHC bound aromatic rings could be easily distinguished from the signals of the corresponding substituents of the amidinate bound aromatic groups. The $C_{NHC}$ in the $^{13}C\{^1H\}$-NMR

 

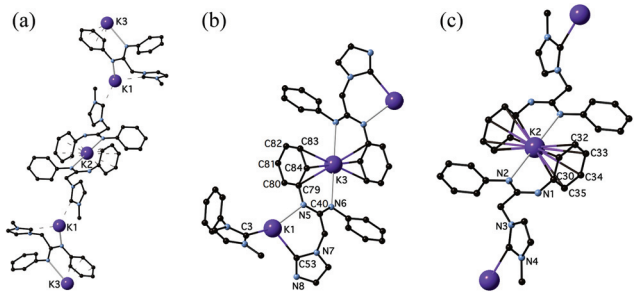


**Fig. 2** (a) Ball-and-stick representation of the one-dimensional structure of **6** showing the different repeat units. Only the *ipso* C of the 2,6-diisopropylphenyl groups at the NHC ring is shown; $Pr^i$ substituents of the 2,6-diisopropylphenyl groups at the amidine N atoms as well as THF solvents of crystallisation are omitted for clarity. (b) Ball-and-stick representation of the coordination environment of K1 and K3. Selected bond lengths (Å) and angles (°): K1–N5 = 2.803(2), K1–C53 = 2.862(3), K3–N6 = 2.946(2), K3–C79 = 3.302(2), K3–C83 = 3.276(3), K3–C84 = 3.146(3). (c) Ball-and-stick representation of the coordination environment of K2. Selected bond lengths (Å) and angles (°): K2–N2 = 3.035(2), K2–C34 = 3.248(2), K2–C33 = 3.256(2), K2–C35 = 3.260(2), K2–C32 = 3.279(2), K2–C30 = 3.307(2).

spectrum was observed at $\delta$ 214.6. In larger scale preparations of **6**, the neutral NHC ligand **5** was not isolated but subjected to the second deprotonation by $KN(SiMe_3)_2$ after separation of the KCl from the reaction mixture by filtration. The salt **6** was crystallised from THF–petrol and its structure was determined crystallographically. It features one-dimensional polymeric 'zig-zag' chains comprising potassium cations, bridged by L as shown in Fig. 2a–c. There are a limited number of structurally characterised potassium amidinates.[30–33] In most reported structures two amidinate ligands adopt a symmetrical $\kappa^1$, $\kappa^1$ coordination bridging two K centers. In the structure of **6** arene ring–potassium interactions, NHC–potassium and $N_{amidinato}$–potassium interactions are involved in the formation of the chain. In this respect, the structure of **6** has similarities with the structure of the potassium bis(2,6-diisopropylphenyl)-formamidinate·*n*THF reported by Junk and Cole.[32]

More specifically, **6** exhibits two types of alternating repeat units in the polymeric chain distinguishable by the different coordination spheres of the potassium centers (Fig. 2b and 2c). In Fig. 2b are shown in detail the coordination environments of K(1) and K(3). K(1) is bound only to one $N_{amidinate}$ and two $C_{NHC}$ atoms [C(3) and C(53)] originating from two NHC functionalities of different ligands L. K(3) is 'sandwiched' by two aromatic rings, and two nitrogen atoms originating from the amidinate end of different ligands that are arranged in a 'tail-to-tail' fashion. Each aromatic ring in proximity to K(3) is nonsymmetrically disposed as evidenced by the K–$C_{aromatic}$ distances: [K(3)–C(83) = 3.276(3) Å, K(3)–C(84) = 3.146(2) Å, K(3)–C(79) = 3.302(2) Å] supporting two $\eta^3$-K(3)–arene interactions with two different aromatic rings.

The coordination sphere of K(2) is shown in Fig. 2c. K(2) is also 'sandwiched' between two aromatic rings arranged in an eclipsed face-to-face stacking. In addition, K(2) is coordinated to two $N_{amidinate}$ donor atoms. The variation of K(2)–$C_{arene}$ distances is small [3.248–3.330 Å, K(2)–arene centroid = 2.967 Å] and possibly dictated by steric factors. All K–$C_{NHC}$ bond distances [in the range between 2.862 and 2.953 Å, see figures] are comparable to those found in the literature (2.810–3.127 Å, average 2.929 Å).[34] All K–$N_{amidinate}$ bonds (2.946–3.035 Å) fall at the long end of the range of anionic potassium–amide bonds found in the CCDC or are even longer (2.578–2.973 Å, average 2.766 Å). All amidinato N atoms are almost planar (angle sums at N atoms *ca.* 355.5–359.5°), while the $C_{amidinato}$–$N_{amidinato}$ (bound to K) and $C_{amidinato}$–$N_{amidinato}$ (unbound) are virtually equal.

### The synthesis of the silver complex 7

Initial insight into the coordination behavior of the ligand HL was sought by the reaction of the imidazolium salt **4** and $Ag_2O$, which is known to provide access to silver complexes with synthetic potential in NHC transmetallation reactions, and could therefore expand the scope and applications of the new ligand design. The metallation took place in refluxing dichloroethane giving complex **7** in good yields (Scheme 5).

Complex **7** was characterised by analytical and spectroscopic methods. An X-ray diffraction study was also performed, however due to the poor crystal and data quality the model serves only to unequivocally establish the atom connectivity in the molecule (Fig. 3) and not to extract accurate metrical data. The ligand is exclusively metallated at the $C_{NHC}$ with dangling amidine functionality. In the crystal the amidine isomer present is *Z-syn* (in contrast to the imidazolium **4** above) possibly in order to reduce steric interactions. The Ag centre adopts an almost linear geometry which is common with analogous compounds previously described.[35] The $^1$H-NMR spectrum of **7** is simpler than that observed for **4** in $CDCl_3$ where the presence of isomers was evident. The methyls of the $Pr^i$ substituents of all the aromatic rings are diastereotopic giving rise to six doublets ($CH(CH_3)_2$) and three septets ($CH(CH_3)_2$). This is in accordance with the presence of one isomer and presumably the persistence of the solid state structure in solution.

### The synthesis of the chromium complexes

The development of new chromium complexes with catalytic potential in the oligomerisation and polymerisation of ethylene and other 1-alkenes is a current topical area in organometallic chemistry. In addition current research is aimed at the elucidation of the operating mechanisms of the above reactions, which are not understood.[36] Having this motive, we decided to prepare Cr complexes with the new ligand with the aim to explore their catalytic potential and reactivity with ethylene. The chromium complexes described below are summarised in Scheme 5.

The reaction of the precursor $[CrCl_2Me(THF)_3]$ with **6** in THF at low temperature gave the purple paramagnetic complex **8** in good yields, which was characterised by X-ray crystallography. A diagram of the molecule is shown in Fig. 4. The metal centre adopts a distorted square-pyramidal geometry with the methyl group [C(51)] at the apical position. The ligand L acts as an anionic bidentate donor ($\kappa^1$-NHC, $\kappa^1$-amidinato *cf.* structure D in Scheme 2) implying that the coordination of the NHC is favored over the imine N atom of the amidinato moiety. A tridentate 'scorpionate' type coordination is also disfavored

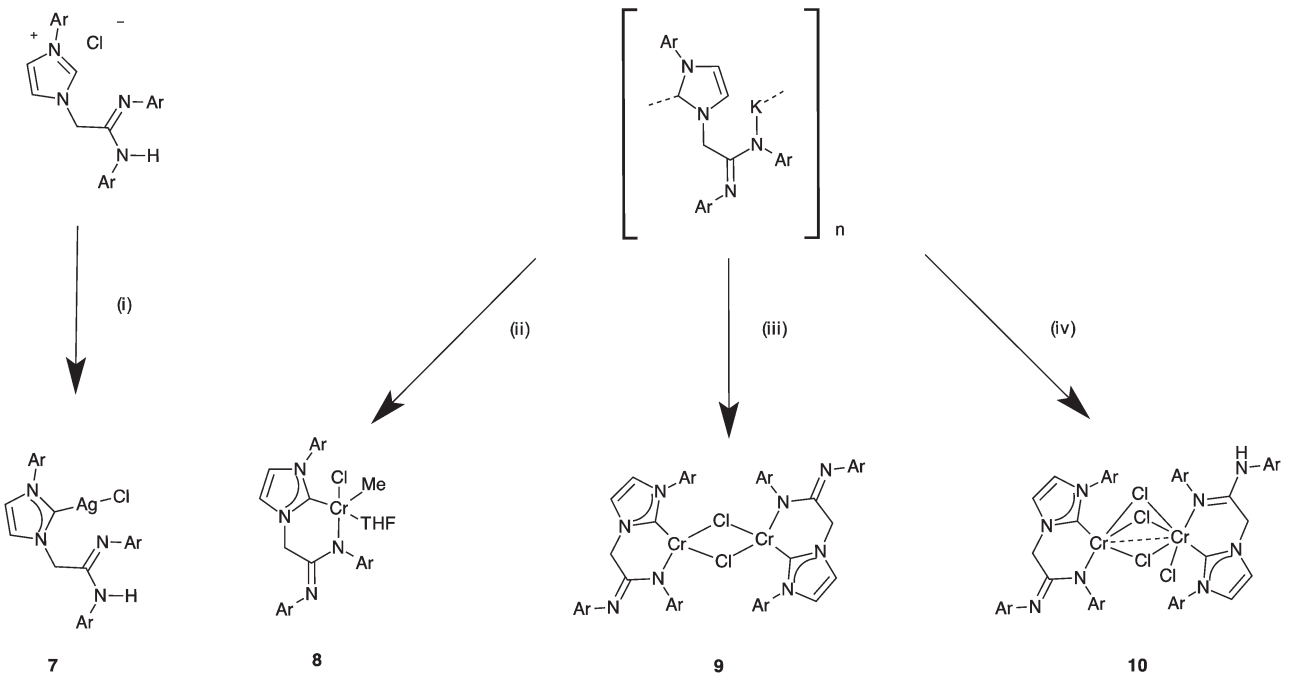


**Scheme 5** Transformations leading to the complexes described in this paper. Reagents and conditions: (i) $Ag_2O$, 1,2-dichloroethane; (ii) 1 equiv. $[CrMeCl_2(THF)_3]$ in THF; (iii) $[CrCl_2(THF)_2]$ in THF; (iv) $[CrCl_3(THF)_3]$ in THF. Ar is 2,6-diisopropylphenyl.

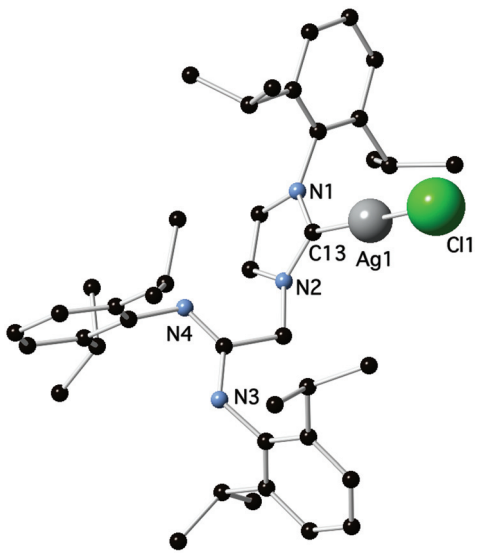


**Fig. 3** Ball-and-stick representation of complex **7**; see text for details.

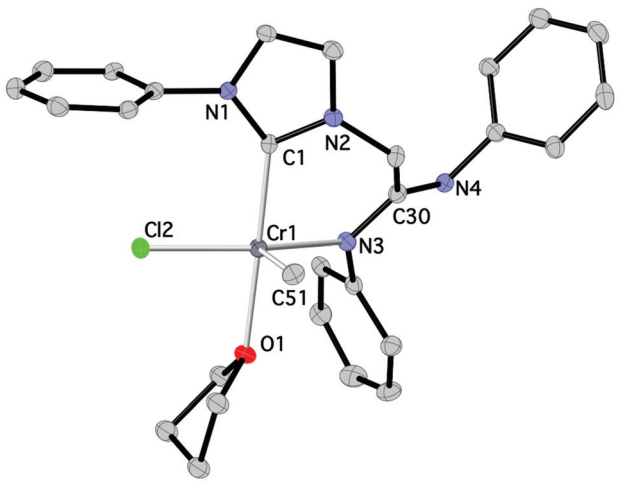


**Fig. 4** Representation of the structure of **8**; ellipsoids are at 30% level. $Pr^i$ substituents of the 2,6-diisopropylphenyl groups are omitted for clarity; only one conformation of the coordinated disordered THF is shown. Selected bond lengths (Å) and angles (°): Cr1–N3 = 2.030(2), Cr1–C51 = 2.055(3), Cr1–C1 = 2.107(3), Cr1–Cl2 = 2.3064(9), N3–C30 = 1.370(4), N4–C30 = 1.290(4), N3–Cr1–C51 = 102.01(12), N3–Cr1–C1 = 88.64(10), C51–Cr1–C1 = 89.25(12).

presumably due to steric reasons. The $C–N_{amidine}$ bond lengths (C30–N3 and C30–N4) give evidence for a localised electronic structure. This coordination mode of the amidinato group is rare with transition metals, in particular electronically unsaturated.[37] The symmetrical chelating bidentate mode has been observed with amidinato ligands in $Cr^{III}$,[4,38] $Cr^{II}$ [39] or with the related 2-amido-pyridines.[40] The $Cr–N_{amidinato}$ at 2.030 Å lies at the long end of the $Cr–N_{amido}$ distance range (1.760–2.080 Å, average 1.845 Å for Cr complexes and 1.803–1.909 Å, average 1.856 Å for $Cr^{III}$ complexes) and is comparable with the bond length in sterically congested terminal $Cr^{II}–NPh_2$. The coordinated $N_{amidinato}$ atom is planar (angle sum 359.4°). The bite angle subtended by the bidentate chelate ligand is 88.6°.

The $Cr–C_{NHC}$ bond length [2.107(3) Å] is in the range reported for other Cr–NHC complexes (2.041–2.245 Å, average 2.134 Å).[41] The difference between the exocyclic [N(1)–C(1)–Cr(1)] and endocyclic [N(2)–C(1)–Cr(1)] angles at the $C_{NHC}$ is 18.8° indicating a trend to release chelate ring strain on coordination and reduced directionality of the $Cr–C_{NHC}$ bond.

 

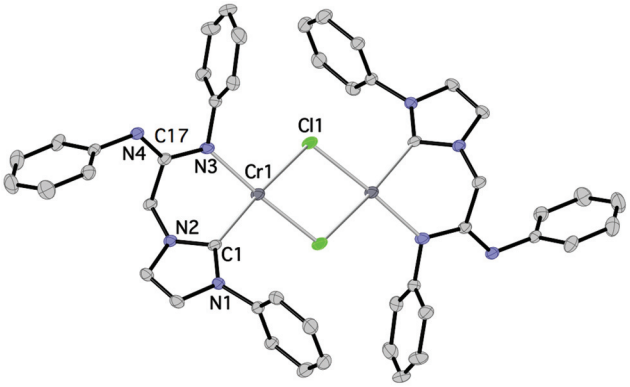


**Fig. 5** Representation of the structure of **9**; ellipsoids are at 30% level. $Pr^i$ substituents of the 2,6-diisopropylphenyl groups are omitted for clarity. Selected bond lengths (Å) and angles (°): Cl1–Cr1 = 2.3884(8), N3–Cr1 = 2.0675(19), C17–N3 = 1.358(3), C17–N4 = 1.296(3), C1–Cr1 = 2.163(2), N3–Cr1–Cl1 = 94.46(6), C1–Cr1–Cl1 = 93.04(6), N3–Cr1–Cl1 = 176.37(6), N3–Cr1-C1 = 90.39(8).

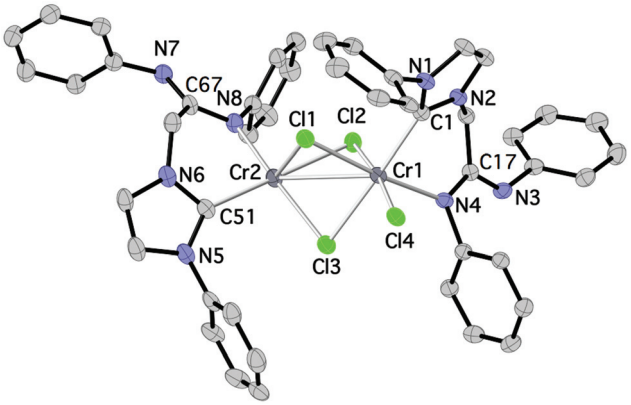


**Fig. 6** Representation of the structure of **10**; ellipsoids are at 30% level. $Pr^i$ substituents of the 2,6-diisopropylphenyl groups and solvent molecules ($CH_2Cl_2$ and ether) present in the asymmetric unit are omitted for clarity. Selected bond lengths (Å) and angles (°): N7–C68 = 1.402(5), N7–C67 = 1.292(5), N3–C17 = 1.342(5), N4–C17 = 1.308(5), Cr2–Cl1 = 2.6311(17), Cr2–Cl2 = 2.4241(16), Cr2–Cl3 = 2.3824(15), Cr2–C51 = 2.120(4), Cr2–N8 = 2.050(3), Cr1–Cl3 = 2.4126(15), Cr1–Cl2 = 2.3996(16), Cr1–Cl1 = 2.3500(17), Cr1–Cl4 = 2.2645(15), Cr1–N4 = 2.124(3), Cr1–C1 = 2.093(4), N8–Cr2–Cl1 = 106.45(10), C51–Cr2–Cl2 = 178.21(10), C51–Cr2–Cl3 = 96.33(12), N8–Cr2–Cl3 = 169.29(10), N8–Cr2–C51 = 89.76(14), N4–Cr1–Cl1 = 172.72(9), C1–Cr1–Cl1 = 92.06(11), N4–Cr1–Cl4 = 93.24(9), C1–Cr1–Cl4 = 94.73(11), C1–Cr1–N4 84.41(13).

The reaction of the precursor $[CrCl_2(THF)_2]$ with **6** in THF at low temperature gave the blue-purple paramagnetic very air sensitive complex **9** in moderate yields. Analytically pure indigo blue powder was isolated by extraction of the reaction residue in diethyl ether, filtration through Celite and removal of the volatiles under reduced pressure. X-ray quality crystals were obtained by slow diffusion of pentane into THF solutions of the complex. The structure of the molecule determined crystallographically is shown in Fig. 5.

Complex **9** is a centrosymmetric dimer with bridging chlorides; here too the ligand L acts as an anionic bidentate donor ($\kappa^1$-NHC, $\kappa^1$-amidinato *cf.* structure D in Scheme 2) with puckered chelate rings. Each metal center adopts a distorted square planar geometry. The C–N distance involving the exocyclic N atoms is shorter (1.296 Å) than the endocyclic (1.358 Å). Both values are comparable to those observed for the corresponding bond lengths in the salt **4** and the complexes **7** and **8** indicating that the ligand π-system is not significantly altered on coordination. The planarity of the coordinated nitrogen (358.5°) supports anionic amide binding, however, the Cr–$N_{amidinato}$ bond length (2.068 Å) is slightly longer than other previously reported terminal $Cr^{II}$–N amides (1.904–2.062 Å, average 1.984 Å). There is no evidence for Cr–Cr interaction (3.619 Å).

Finally, the reaction of **6** with $[CrCl_3(THF)_3]$ gave the paramagnetic air sensitive complex **10** in good yields. Crystals of **10** were obtained from $CH_2Cl_2$–ether and studied by single crystal X-ray diffraction. A diagram of the molecule is shown in Fig. 6.

The binuclear complex comprises two different metal centers: Cr1 is coordinated by six donors in a distorted octahedral geometry and Cr2 by five donors in a distorted trigonal bipyramidal geometry. The amidinato ligand acts again as bidentate *via* the NHC and one nitrogen atom of the amidine functionality. Careful perusal of the metrical data shows additional subtle differences. The bidentate ligand at Cr2 features exocyclic and endocyclic C–N and Cr–N bond lengths (1.292 Å, 1.340 Å, and 2.050 Å, respectively) comparable to those in complexes **8** and **9**. Consequently, the coordination mode is analogous and described by structure D in Scheme 2. In contrast, the bidentate ligand at Cr1 features exocyclic and endocyclic C–N and Cr–N bond lengths at 1.308 Å, 1.340 Å and 2.125 Å, respectively, which support a coordination mode best described by the structure E in Scheme 2, and the involvement of a neutral amidine ligand (HL). Therefore, the two metal centers Cr1 and Cr2 are in oxidation states III and II, respectively. This is further supported by the Cr–$C_{NHC}$ bond lengths (Cr1–C 2.093 Å and Cr2–C 2.120 Å) which are significantly different and in line with the trend observed for **8** (2.107 Å) and **9** (2.164 Å), respectively. Interestingly, in **10** the intermetallic distance is much shorter (3.109 Å). The mechanism of formation of **10** has not been elucidated. It is plausible to postulate that the initial formation of a $(CrCl_2L)_n$, $n$ = 1,2, by a salt metathetical reaction is followed by protonation of an anionic amidinato group. The source of the proton may be THF or solvents of crystallisation.

Preliminary catalytic testing using complexes **8** and **9** for the oligomerisation/polymerisation of ethylene was carried out in the presence of $EtAlCl_2$ as an activator. The results show that **8** is a low activity polymerisation catalyst, while **9** was inactive. However, the latter may be decomposing before the catalytic reaction as indicated by the color change observed after dissolving it in chlorobenzene, the solvent of choice for the catalytic experiments. Further catalytic studies are underway.

In conclusion, we have introduced a novel NHC functionalisation strategy involving the versatile amidine functionality. The easy availability of well defined ligand transfer reagents (neutral ligand HL, silver complex Ag(HL) and the KL) provides options for the synthesis of complexes with metals of different nature in various environments and oxidation states. The new ligand systems exhibit a range of coordination modes (monodentate, bidentate and bridging) which have been observed crystallographically with the metals used in the present study. We are now focussing our efforts on the exploration of the scope of the

mixed donor amidine NHCs across the periodic table, the development and refinement of analogous systems with pendant arms at the N-termini of the amidine, guanidine functionalisation and selected catalytic applications of complexes with the new ligand designs.

## Experimental section

Elemental analyses were carried out by the London Metropolitan University microanalytical laboratory. All manipulations involving metals were performed under nitrogen in a Braun glove box or using standard Schlenk techniques, unless stated otherwise. Solvents were dried by passing through alumina columns (pentane, toluene) or by distillation from sodium benzophenone ketyl (ether, THF) and kept under Ar over carefully activated sieves until use. NMR solvents were dried and distilled from KH and stored in the glove box over activated molecular sieves. The starting materials *N*,*N*′-bis(2,6-diisopropylphenyl)-chloroacetamide[42] and $[MeCrCl_2(THF)_3]$[43] were prepared according to the literature procedures. $[CrCl_2(THF)_2]$ was prepared by continuous Soxhlet extraction of commercial anhydrous $[CrCl_2]$ (Aldrich) with THF for 48 h.

NMR data were recorded on Bruker AV 300 and DPX-400 spectrometers, operating at 300 and 400 MHz ($^1$H), respectively. The spectra were referenced internally using the signal from the residual protio-solvent ($^1$H) or the signals of the solvent ($^{13}$C).

### 2-Chloro-*N*,*N*′-bis(2,6-diisopropylphenyl)acetamidine 3

A modification of the method published by Wolmershäuser is followed.[28] The imidoyl chloride was isolated and reacted in a separate step with 2,6-diisopropylaniline to form the chloromethylamidines.

To a suspension of 2-chloro-*N*-(2,6-diisopropylphenyl)acetamide (31.72 g, 0.120 mol) in dry benzene (*ca.* 100 cm$^3$) was added *portionwise* at room temperature solid $PCl_5$ (28.53 g, 0.137 mol). Gas evolution (HCl) took place following the addition of each portion. After the completion of the addition the mixture was slowly brought to reflux (oil bath temperature 75–80 °C) and kept at this until no further HCl evolution through the bubbler is noticeable (usually 20–30 min). The reflux condenser was replaced by a distillation head equipped with a short (10 cm) fractionation column. The benzene was removed at atmospheric pressure, followed by the $POCl_3$ at reduced pressure and finally the imidoyl chloride **2** as an off white liquid (82–84 °C, 0.36 mbar). Yield: 27.75 g, 85%. The product **2** can be stored in Youngs' ampoules under $N_2$. $^1$H NMR ($CDCl_3$): $\delta$ 1.28 (d, 12H, $CH_3$)$_2$CH), 2.83 (septet, 2H, ($CH_3$)$_2$C*H*), 4.61 (s, 2H, C$H_2$Cl), 7.2–7.4 (m, 4H, aromatics).

2,6-Diisopropylaniline (19 g, 0.105 mol) in benzene (75 cm$^3$) was added to a solution of the imidoyl chloride **2** (27.2 g, 0.10 mol) in benzene (75 cm$^3$) and the reaction mixture was refluxed for 20 h. After cooling a white precipitate appeared which was washed with petrol. To liberate the free amidine base the solid was dissolved in ethanol (250 cm$^3$) and treated with aqueous ammonia (25%, 6 × 60 cm$^3$). The solid product was collected by filtration, recrystallised from ethanol and dried under reduced pressure to give small white crystals of **3**. Yield: 31.15 g, 72%. $^1$H-NMR ($CDCl_3$, 300 MHz): (mixture of *E*/*Z* isomers) 7.28–6.88 (6H, m, H-aromatic); 6.11 (0.6H, s, N*H*), 5.35 (0.4H, s, N*H*); 3.96 (1.2H, s, C$H_2$Cl); 3.89 (0.8, sC$H_2$Cl); 3.25 (1.2H, sept, $J$ = 7.5 Hz, C*H*($CH_3$)$_2$); 3.09 (2H, sept, $J$ = 7.5 Hz, C*H*($CH_3$)$_2$); 2.81 (0.8H, sept, $J$ = 7.5 Hz, C*H*($CH_3$)$_2$); 1.20–0.91 (24H, m, CH(C$H_3$)$_2$). $^{13}$C{$^1$H}-NMR ($CDCl_3$, 75 MHz): 151.7; 150.7; 147.2; 147.0; 143.8; 139.2; 138.9; 132.8; 132. 2; 128.9; 128.2; 123.9; 123.8; 123.3; 123.1; 123.0; 40.8 (–*C*H$_2$–); 39.3 (–*C*H$_2$–); 28.7; 28.3; 28.2; 27.7; 25.3; 24.3; 23.8; 23.7; 22.8; 22.4. M.S. (ES$^+$): 415.6 (M + H)$^+$; 413.5 (M + H)$^+$.

### 3-(2,6-Diisopropylphenyl)-1-[*N*,*N*′-bis(2,6-diisopropylphenyl)-acetamidyl]imidazolium chloride 4

2-Chloro-*N*,*N*′-bis(2,6-diisopropylphenyl)acetimidamide **3** (20 g, 50 mmol) and 2,6-diisopropylphenylimidazol (12.56 g, 55 mmol) were heated in a sealed Youngs' ampoule under partial vacuum at 150 °C for 4 days. The resulting material was dissolved in the minimum amount of $CH_2Cl_2$ and triturated with diethyl ether to give a white solid which was dried azeotropically with toluene. It was finally washed with dry diethyl ether, dried under vacuum and stored in the glove box. Yield: 19.69 g, 65%. X-ray quality crystals were obtained by layering with diethyl ether a concentrated $CH_2Cl_2$ solution. $^1$H-NMR ($CDCl_3$, 300 MHz): (mixture of *E*/*Z* isomers) 10.95 (0.4H, s, imidazolium-H); 10.91 (0.6H, s, imidazolium-H); 9.69 (0.4H, s, N*H*); 7.50 (0.4H, t, $J$ = 6 Hz, aromatic-H); 7.40 (0.6 H, t, $J$ = 6 Hz, aromatic-H); 7.30–6.90 (8 H, m, aromatic-H and 0.8 H NHC-backbone); 6.90 (0.6 H, broad s, NHC-backbone); 6.05 (0.6 H, broad s, NHC-backbone); 5.53 (0.6 H, s, N*H*); 5.49 (0.8, s, C$H_2$); 5.49 (1.2, s, C$H_2$); 3.30–3.11 (2H, m, C*H*($CH_3$)$_2$); 2.95 (1.2H, two overlapped sept, $J$ = 6.5 Hz, C*H*($CH_3$)$_2$); 2.81 (0.8H, sept, $J$ = 6.5 Hz, C*H*($CH_3$)$_2$); 2.35 (1.2H, sept, $J$ = 6.5 Hz, C*H*-($CH_3$)$_2$); 2.15 (0.8H, sept, $J$ = 6.5 Hz, C*H*($CH_3$)$_2$); 1.40, 1.35, 1.30, 1.15, 1.10, 1.00 and 0.90 (36H, d (some are overlapping), $J$ = 6.5 Hz, CH(C$H_3$)$_2$). $^{13}$C{$^1$H}-NMR ($CDCl_3$, 300 MHz): 148.7; 147.2; 146.6; 145.6; 145.1; 142.3; 142.0; 139.5; 139.0; 138.7; 133.4; 132.1; 131.7; 130.8; 130.4; 130.1; 129.5; 127.6; 124.8; 124.5; 124.3; 124.1; 123.9; 123.2; 123.2; 123.0; 122.9; 122.7; 65.8; 49.6 (–*C*H$_2$–); 46.1 (–*C*H$_2$–); 29.0; 28.7; 28.6; 28.5; 28.3; 25.8; 25.0; 24.5; 24.4; 24.3; 24.1; 24.0; 23.3; 22.3; 22.2; 21.8; 15.3. $^1$H-NMR (d$_6$-DMSO, 300 MHz): 9.62 (1H, s, imidazolium-H); 8.11 (1H, s broad, NHC-backbone); 7.77 (1H, s broad, NHC-backbone); 7.70–6.95 (9H, m, aromatic-H); 4.70 (2H, s, C$H_2$); 3.25 (2H, sept, $J$ = 7.5 Hz, C*H*($CH_3$)$_2$); 2.95 (2H, sept, $J$ = 7.5 Hz, C*H*($CH_3$)$_2$); 2.30 (2H, sept, $J$ = 7.5 Hz, C*H*-($CH_3$)$_2$); 1.38 (6H, d, $J$ = 7 Hz, CH(C$H_3$)$_2$); 1.33 (6H, d, $J$ = 7 Hz, CH(C$H_3$)$_2$); 1.20–0.90 (24H, m, CH(C$H_3$)$_2$). $^{13}$C{$^1$H}-NMR (d$_6$-DMSO, 75 MHz): 147.4; 146.9; 145.1; 142.9; 139.9; 137.9; 132.5; 131.4; 130.5; 128.5; 124.3; 123.7; 122.7; 122.6; 49.6 (*C*H$_2$); 27.8; 27.7; 24.4; 23.9; 23.5; 22.9; 22.4. M.S. (ES$^+$): 607.7 (M − Cl)$^+$; 606.7 (M − Cl)$^+$; 605.7 (M − Cl)$^+$.

### Deprotonation procedures

**3-(2,6-Diisopropylphenyl)-1-[*N*,*N*′-bis(2,6-diisopropylphenyl)-acetamidyl]imidazol-2-ylidene 5.** The imidazolium chloride **4**

 

(1.88 g, 3 mmol) was combined with 1 equiv. of $KN(SiMe_3)_2$ (0.60 g, 3 mmol) in benzene (20 $cm^3$) and the yellow suspension was stirred overnight. The precipitated KCl was removed by filtration through Celite and the solution was evaporated to dryness. The yellow air sensitive solid was characterised by NMR spectroscopy. $^1$H-NMR ($C_6D_6$): 8.05 (1H, broad s, N*H*); 7.20–6.85 (9H, m, H-aromatic); 6.30 and 6.15 (2H, d, $J$ = 6.5 Hz, NHC-backbone); 4.45 (2H, s, C$H_2$); 3.50 (2H, sept, $J$ = 7.5 Hz, C$H$(CH$_3$)$_2$); 3.25 (2H, sept, $J$ = 7.5 Hz, C$H$(CH$_3$)$_2$); 2.65 (2H, sept, $J$ = 7.5 Hz, C$H$(CH$_3$)$_2$); 1.35–0.8 (36H, m, CH(C$H_3$)$_2$). $^{13}$C{$^1$H}-NMR $C_6D_6$: 217.0 (NHC-*C*); 150.9; 145.7; 145.1; 144.3; 137.7; 136.8; 133.1; 127.8; 122.5; 122.0; 121.8; 120.9; 119.0; 48.4 (–*C*H$_2$–); 27.7; 26.9; 26.8; 23.0; 22.9; 22.8; 22.4; 21.6.

**3-(2,6-Diisopropylphenyl)-1-[2-*N*,*N*′bis(2,6-diisopropylphenylamidinate)ethyl]imidazol-2-ylidene potassium 6.** The imidazolium chloride **4** (1.88 g, 3 mmol) was combined with 1 equiv. of $KN(SiMe_3)_2$ (0.60 g, 3 mmol) in benzene (20 $cm^3$) and the yellow suspension was stirred overnight. The precipitated KCl was removed by filtration through Celite and the solution of the ligand **5** was subjected to a second deprotonation with an additional equivalent of $KN(SiMe_3)_2$ (0.60 g, 3 mmol) in benzene (20 $cm^3$). The orange suspension was stirred overnight. The precipitated extremely air sensitive, beige product **6** was isolated on a frit, washed with benzene (2 $cm^3$) and pentane (10 $cm^3$) and dried under vacuum. Yield: 1.15 g, 61%. X-ray quality crystals were obtained by layering a concentrated THF solution of **6** with pentane. Elemental analysis: Calculated for $C_{43}H_{59}N_4K_1$·0.5 THF (%): C, 75.99; H, 8.69; N 8.25. Found (%): C, 76.09; H, 8.67; N, 8.95. $^1$H-NMR ($d_5$-pyridine, 300 MHz): 7.45–7.00 (11H, m, aromatic-H and NHC carbene backbone); 4.95 (2H, s, C$H_2$); 3.76 (4H, m, C$H$(CH$_3$)$_2$); 2.91 (2H, m, C$H$(CH$_3$)$_2$); 1.35–0.89 (36H, m, CH(C$H_3$)$_2$). $^{13}$C{$^1$H}-NMR ($d_5$-pyridine, 75 MHz): 214.6 (NHC); 165.1; 156.8; 156.3; 147.3; 142.4; 140.1; 138.4; 129.2; 122.7; 121.2; 119.98; 53.71; 51.37; 28.7; 28.5; 25.4; 25.0; 24.8; 24.4; 24.1.

### Silver complex 7

$Ag_2O$ (0.54 g, 2.3 mmol) was added to a solution of **4** (1.00 g, 1.5 mmol) in 1,2-dichloroethane (50 $cm^3$). The mixture was refluxed for 20 h and after cooling to room temperature, the black suspension was filtered through Celite. Removal of the volatiles under reduced pressure and dissolving the residue in the minimal amount of $CH_2Cl_2$ (5 $cm^3$), precipitation with diethyl ether (20 $cm^3$) and filtration of the resulting colorless solid gave **7** which was washed with diethyl ether (3 × 15 $cm^3$) and dried under vacuum. Yield: 0.40 g, 53%. Elemental analysis: Calculated for $C_{41}H_{56}N_4AgCl$ (%): C, 65.81, H, 7.54, N, 7.49. Found (%): C, 65.89; H, 7.76; N, 8.49. $^1$H-NMR ($CDCl_3$, 300 MHz): 7.35 (1H, t, $J$ = 9 Hz, C-H aromatic); 7.20 (1H, t, $J$ = 9 Hz, C-H aromatic); 7.19–7.09 (7H, m, C-H aromatic); 7.00 (1H, dd, $J$ = 6 Hz, NHC-backbone); 6.88 (1H, dd, $J$ = 3 Hz, NHC-backbone); 5.46 (1H, s, N*H*); 4.69 (2H, s, $CH_2$-bridge); 3.20 (2H, sept, $J$ = 6 Hz, C$H$(CH$_3$)$_2$); 2.98 (2H, sept, $J$ = 6 Hz, C$H$(CH$_3$)$_2$); 2.37 (2H, sept, $J$ = 6 Hz, C$H$(CH$_3$)$_2$); 1.39 (6H, d, $J$ = 6 Hz, CH(C$H_3$)$_2$); 1.29 (6H, d, $J$ = 6 Hz, CH(C$H_3$)$_2$); 1.08 (6H, d, $J$ = 6 Hz, CH(C$H_3$)$_2$); 1.03 (6H, d, $J$ = 6 Hz, CH(C$H_3$)$_2$); 1.02 (6H, d, $J$ = 6 Hz, CH(C$H_3$)$_2$); 0.96 (6H, d, $J$ = 6 Hz, CH(C$H_3$)$_2$). $^{13}$C{$^1$H}-NMR ($CDCl_3$, 75 MHz): 148.8; 147.1; 145.8; 142.9; 138.6; 134.7; 131.2; 130.4; 129.4; 124.3; 124.2; 123.1; 122.2; 122.1; 52.0; 35.1; 28.8; 28.6; 28.1; 24.8; 24.5; 24.3; 24.2; 23.6; 21.7.

### Complex 8

A precooled (−78 °C) solution of **6** (0.30 g, 0.47 mmol) in THF (30 $cm^3$) was added to a solution of $[CrCl_2Me(THF)_3]$ in THF (20 $cm^3$) at −78 °C. The light green reaction mixture was allowed to reach room temperature and stirred for 1 h when the colour turned to purple. The volatiles were removed under reduced pressure, the residue extracted with toluene and filtered through Celite. Evaporation of the solvent under reduced pressure gave the analytically pure **8** as purple powder. Yield: 0.19 g, 58%. X-ray quality crystals were obtained by slow diffusion of petrol in a concentrated diethyl ether solution. Elemental analysis: Calculated (%) for (M − THF) $C_{42}H_{58}ClCrN_4$: C, 71.31; H, 8.41; N, 7.92. Found (%): C, 71.33; H, 8.17; N, 7.83. The $^1$H-NMR spectrum of **8** is broad and featureless.

### Complex 9

A pre-cooled (−78 °C) solution of **6** (0.30 g, 0.47 mmol) in THF (30 $cm^3$) was added to a solution of $[CrCl_2(THF)_2]$ in the same solvent (20 $cm^3$) at −78 °C. The light grey-green reaction mixture was allowed to reach room temperature and stirred for 1 h when it became indigo. The solution was concentrated to *ca.* 10 $cm^3$ and filtered through Celite. Slow diffusion of pentane into the THF gave dark blue-purple prisms. Yield: 0.12 g, 36%. Elemental analysis: Calculated for $C_{82}H_{110}N_8Cr_2Cl_2$ (%): C, 71.12; H, 8.15; N, 8.09. Found (%): C, 71.15; H, 8.02; N, 8.10.

### Complex 10

A precooled (−78 °C) solution of **6** (1.00 g, 1.56 mmol) in THF (20 $cm^3$) was added to a solution of $[CrCl_3(THF)_3]$ in the same solvent (20 $cm^3$) and temperature. The mixture was allowed to reach room temperature and stirred overnight. During this time it turned from purple to brown. THF was removed under reduced pressure, the residue extracted with toluene and filtered through Celite. Removal of the volatiles under reduced pressure gave the analytically pure product in almost quantitative yield. Yield: 1.10 g, 97%. The product can be crystallized by slow diffusion of ether in a concentrated $CH_2Cl_2$ solution. Elemental analysis: Calculated for $C_{82}H_{111}N_8Cr_2Cl_4$ (%): C, 67.76; H, 7.57; N, 7.71. Found (%): C, 67.78; H, 7.64; N, 7.81.

### X-ray crystallography

A summary of the crystal data, data collection and refinement for complexes **4**, **6**, **7**, **8**, **9** and **10** is given in Table 1. The crystals were mounted on a glass fiber with grease, from Fomblin vacuum oil.

Data sets for **4**, **6**, **7** and **8** were collected on an Enraf-Nonius Kappa CCD area detector diffractometer with an FR591 rotating anode (Mo-Kα radiation) and an Oxford Cryosystems low

**Table 1** Crystal data for complexes **4**, **6**, **7**, **8**, **9** and **10**

| | **4** | **6** | **7** | **8** | **9** | **10** |
|---|---|---|---|---|---|---|
| Chemical formula | $C_{41}H_{57}ClN_4 \cdot 1.5CHCl_3$ | $C_{43}H_{59}KN_4O_{0.5}$ CCDC | $C_{41}H_{56}AgClN_4$ CCDC | $C_{46}H_{66}ClCrN_4O$ CCDC | $C_{82}H_{110}Cl_2Cr_2N_8$ CCDC | $C_{82}H_{112}Cl_4Cr_2N_8 \cdot C_4H_{10}O \cdot 2(CH_2Cl_2)$ |
| Formula mass | 820.41 | 679.04 | 748.22 | 778.48 | 1382.68 | 1699.57 |
| Crystal system | Monoclinic | Triclinic | Triclinic | Orthorhombic | Monoclinic | Monoclinic |
| $a$/Å | 22.5237(3) | 13.80520(10) | 10.2894(7) | 14.4973(4) | 12.2847(9) | 14.433(10) |
| $b$/Å | 12.7743(2) | 14.34640(10) | 12.4817(13) | 16.0212(4) | 15.9373(11) | 21.648(15) |
| $c$/Å | 16.6305(2) | 20.6098(2) | 16.3801(17) | 18.7006(4) | 22.3137(13) | 29.447(19) |
| $\alpha$/° | 90.00 | 90.5980(10) | 80.103(4) | 90.00 | 90.00 | 90.00 |
| $\beta$/° | 102.6610(10) | 94.8700(10) | 86.108(5) | 90.00 | 119.069(3) | 97.642(7) |
| $\gamma$/° | 90.00 | 95.8140(10) | 74.035(5) | 90.00 | 90.00 | 90.00 |
| Unit cell volume/Å$^3$ | 5591 | 4045.47(6) | 748.22 | 4343.48(19) | 3818.4(4) | 1699.57 |
| Temperature/K | 120(2) | 120(2) | 120(2) | 120(2) | 120(2) | 120(2) |
| Space group | *Cc* | $P\bar{1}$ | $P\bar{1}$ | *P*212121 | *P*21/*c* | *P*21/*c* |
| Formula units/cell, $Z$ | 4 | 4 | 2 | 4 | 2 | 4 |
| Absorption coefficient, $\mu$/mm$^{-1}$ | 0.371 | 0.166 | 0.605 | 0.363 | 0.402 | 0.520 |
| No. of reflections measured | 50 959 | 18 443 | 8364 | 9596 | 11 240 | 15 908 |
| No. of independent reflections | 5357 | 13 353 | 3367 | 7847 | 5891 | 9457 |
| $R_{int}$ | 0.0537 | 0.0565 | 0.2321 | 0.0625 | 0.0698 | 0.0908 |
| Final $R_1$ values ($I > 2\sigma(I)$) | 0.0495 | 0.0722 | 0.0702 | 0.0520 | 0.0568 | 0.0670 |
| Final w$R(F^2)$ values ($I > 2\sigma(I)$) | 0.1387 | 0.1516 | 0.1191 | 0.0962 | 0.1301 | 0.1778 |
| Final $R_1$ values (all data) | 0.0615 | 0.1081 | 0.2433 | 0.0752 | 0.1384 | 0.1224 |
| Final w$R(F^2)$ values (all data) | 0.1439 | 0.1739 | 0.1637 | 0.1069 | 0.1653 | 0.2097 |
| Goodness of fit on $F^2$ | 1.045 | 1.081 | 0.937 | 1.075 | 0.993 | 1.026 |

temperature device operating in $\omega$ scanning mode with $\psi$ and $\omega$ scans to fill the Ewald sphere. The programs used for control and integration were Collect,[44] Scalepack, and Denzo.[45] All non-hydrogen atoms were refined using anisotropic thermal parameters, and hydrogens were added using a riding model.

The data set for **9** was collected on a Bruker APEX II DUO Kappa-CCD diffractometer equipped with an Oxford Cryosystem liquid $N_2$ device, using Mo-K$\alpha$ radiation ($\lambda$ = 0.71073 Å). The crystal–detector distance was 38 mm. The cell parameters were determined (APEX2 software)[46] from reflections taken from three sets of 12 frames, each at 10 s exposure. All solutions and refinements were performed either using the WinGX[47] package and all software packages within, or the program SHELXS-97.[48] The refinement and all further calculations were carried out using SHELXL- 97.[49] The H-atoms were included in calculated positions and treated as riding atoms using SHELXL default parameters. The non-H atoms were refined anisotropically, using weighted full-matrix least-squares on $F^2$. The crystals of complex **10** were very small and the data set was collected at the synchrotron facility at Darebury, UK.[50]

## Acknowledgements

We thank Sasol Technology UK for the financial support of this project (studentship to S.C.-G.) and the C.N.R.S. for a fellowship (to A.A.D.). A.A.D. is also grateful to the Région Alsace, the Département du Bas-Rhin and the Communauté Urbaine de Strasbourg for the award of a Gutenberg Excellence Chair (2010–2011). We also thank Dr Mark E. Light, Simon J. Coles (University of Southampton) and Dr Lydia Berlot (Universitè de Strasbourg) for assistance with crystallographic data collection and structure determination.

## References

1 (*a*) A. W. Coleman, P. B. Hitchcock, M. F. Lappert, R. K. Maskell and J. H. Müller, *J. Organomet. Chem.*, 1985, **296**, 173–196; (*b*) J. A. Chamizo and M. F. Lappert, *J. Org. Chem.*, 1989, **54**, 4684–4686.
2 W. A. Herrmann, C. Köcher, L. J. Gooßen and G. R. J. Artus, *Chem.–Eur. J.*, 1996, **2**, 1627–1636.
3 O. Kühl, *Functionalized N-Heterocyclic Carbene Complexes*, Wiley, Chichester, 2010.
4 O. M. El-Kadri, M. J. Heeg and C. H. Winter, *Dalton Trans.*, 2006, 4506–4513.
5 A. A. D. Tulloch, S. Winston, A. A. Danopoulos, G. Eastham and M. B. Hursthouse, *Dalton Trans.*, 2003, 699–708.
6 S. Dastgir, K. S. Coleman, A. R. Cowley and M. L. H. Green, *Organometallics*, 2005, **25**, 300–306.
7 M. K. Samantaray, M. M. Shaikh and P. Ghosh, *Organometallics*, 2009, **28**, 2267–2275.
8 I. S. Edworthy, A. J. Blake, C. Wilson and P. L. Arnold, *Organometallics*, 2007, **26**, 3684–3689.
9 R. E. Douthwaite, J. Houghton and B. M. Kariuki, *Chem. Commun.*, 2004, 698–699.
10 L. P. Spencer, C. Beddie, M. B. Hall and M. D. Fryzuk, *J. Am. Chem. Soc.*, 2006, **128**, 12531–12543.
11 F. T. Edelmann, in *Advances in Organometallic Chemistry*, Academic Press, 2008, vol. 57, pp. 183–352.
12 (*a*) S. Collins, *Coord. Chem. Rev.*, 2011, **255**, 118–138; (*b*) E. Smolensky and M. S. Eisen, *Dalton Trans.*, 2007, 5623–5650.

 

13 F. T. Edelmann, *Chem. Soc. Rev.*, 2012, DOI: 10.1039/C2CS35180C.
14 P. C. Junk and M. L. Cole, *Chem. Commun.*, 2007, 1579–1590.
15 C. L. Perrin, in *The Chemistry of Functional Groups: Amidines*, ed. S. Patai and Z. Pappoport, Wiley and Sons, Chichester, 1991, vol. 2.
16 M. P. Coles, *Dalton Trans.*, 2006, 985–1001.
17 S. Bambirra, M. J. R. Brandsma, E. A. C. Brussee, A. Meetsma, B. Hessen and J. H. Teuben, *Organometallics*, 2000, **19**, 3197–3204.
18 A. V. Makarycheva-Mikhailova, V. Y. Kukushkin, A. A. Nazarov, D. A. Garnovskii, A. J. L. Pombeiro, M. Haukka, B. K. Keppler and M. Galanski, *Inorg. Chem.*, 2003, **42**, 2805–2813.
19 K. Kincaid, C. P. Gerlach, G. R. Giesbrecht, J. R. Hagadorn, G. D. Whitener, A. Shafir and J. Arnold, *Organometallics*, 1999, **18**, 5360–5366.
20 T. J. J. Sciarone, C. A. Nijhuis, A. Meetsma and B. Hessen, *Organometallics*, 2008, **27**, 2058–2065.
21 K. Multani, L. J. E. Stanlake and D. W. Stephan, *Dalton Trans.*, 2010, **39**, 8957–8966.
22 M.-T. Chen, K.-M. Wu and C.-T. Chen, *Eur. J. Inorg. Chem.*, 2012, **2012**, 720–726.
23 E. Rabinovich, S. Aharonovich, M. Botoshansky and M. S. Eisen, *Dalton Trans.*, 2010, 6667–6676.
24 S. Aharonovich, M. Botoshanski, Z. Rabinovich, R. M. Waymouth and M. S. Eisen, *Inorg. Chem.*, 2009, **49**, 1220–1229.
25 Z.-J. Yao, G. Su and G.-X. Jin, *Chem.–Eur. J.*, 2011, **17**, 13298–13307.
26 M. Sinenkov, E. Kirillov, T. Roisnel, G. Fukin, A. Trifonov and J.-F. Carpentier, *Organometallics*, 2011, **30**, 5509–5523.
27 A. Otero, J. Fernández-Baeza, A. Antiñolo, J. Tejeda, A. n. Lara-Sánchez, L. F. Sánchez-Barba, I. López-Solera and A. M. Rodriguez, *Inorg. Chem.*, 2007, **46**, 1760–1770.
28 R. T. Boere, V. Klassen and G. Wolmershäuser, *J. Chem. Soc., Dalton Trans.*, 1998, 4147–4154.
29 See ref. 15.
30 P. B. Hitchcock, M. F. Lappert and M. Layh, *J. Chem. Soc., Dalton Trans*, 1998, 3113–3118.
31 P. B. Hitchcock, M. F. Lappert and D.-S. Liu, *J. Organomet. Chem.*, 1995, **488**, 241–248.
32 M. L. Cole and P. C. Junk, *J. Organomet. Chem.*, 2003, **666**, 55–62.
33 (*a*) J. Baldamus, C. Berghof, M. L. Cole, D. J. Evans, E. Hey-Hawkins and P. C. Junk, *J. Chem. Soc., Dalton Trans.*, 2002, 4185–4192; (*b*) J. Baldamus, C. Berghof, M. L. Cole, D. J. Evans, E. Hey-Hawkins and P. C. Junk, *J. Chem. Soc., Dalton Trans.*, 2002, 2802–2804.
34 (*a*) S. P. Downing and A. A. Danopoulos, *Organometallics*, 2006, **25**, 1337–1340; (*b*) L. Arnold, M. Rodden and C. Wilson, *Chem. Commun.*, 2005, 1743–1745; (*c*) M. S. Hill, G. Kociok-Köhn and D. J. MacDougall, *Inorg. Chem.*, 2011, **50**, 5234–5241.
35 J. C. Garrison and W. J. Youngs, *Chem. Rev.*, 2005, **105**, 3978–4008.
36 D. S. McGuinness, *Chem. Rev.*, 2010, **111**, 2321–2341.
37 (*a*) D. Liguori, R. Centore, Z. Csok and A. Tuzi, *Macromol. Chem. Phys.*, 2004, **205**, 1058–1063; (*b*) R. P. Rose, C. Jones, C. Schulten, S. Aldridge and A. Stasch, *Chem.–Eur. J.*, 2008, **14**, 8477–8480. cH. Shen, H.-S. Chan and Z. Xie, *J. Am. Chem. Soc.*, 2007, **129**, 12934–12935.
38 C.-W. Hsu, J.-S. K. Yu, C.-H. Yen, G.-H. Lee, Y. Wang and Y.-C. Tsai, *Angew. Chem., Int. Ed.*, 2008, **47**, 9933–9936.
39 (*a*) F. A. Cotton, L. M. Daniels, C. A. Murillo and P. Schooler, *J. Chem. Soc., Dalton Trans.*, 2000, 2001–2005; (*b*) C. A. Nijhuis, E. Jellema, T. J. J. Sciarone, A. Meetsma, P. H. M. Budzelaar and B. Hessen, *Eur. J. Inorg. Chem.*, 2005, **2005**, 2089–2099.
40 (*a*) A. Noor, G. Glatz, R. Müller, M. Kaupp, S. Demeshko and R. Kempe, *Nat. Chem.*, 2009, **1**, 322–325; (*b*) A. Noor, F. R. Wagner and R. Kempe, *Angew. Chem.,Int. Ed.*, 2008, **47**, 7246–7249.
41 S. Conde-Guadano, A. A. Danopoulos, R. Pattacini, M. Hanton and R. P. Tooze, *Organometallics*, 2012, **31**, 1643–1652.
42 S. H. Park, H. J. Gwon, J. S. Park and K. B. Park, *QSAR Comb. Sci.*, 2004, **23**, 868–874.
43 K. Nishimura, H. Kuribayashi, A. Yamamoto and S. Ikeda, *J. Organomet. Chem.*, 1972, **37**, 317–329.
44 Nonius BV, Delft, The Netherlands, 1997–2000.
45 Z. Otwinowski and W. Minor, in *Macromolecular Crystallography, Part A*, ed. C. W. Carter, Jr. and R. M. Sweet, 1997, vol. 276, pp. 307–326.
46 Bruker AXS Inc, Madison, USA, 2006.
47 L. J. Farrugia, *J. Appl. Crystallogr.*, 1999, **32**, 83.
48 G. M. Sheldrick, Universität Göttingen, Göttingen Germany, 1999.
49 G. M. Sheldrick, *Acta Crystallogr., Sect. A: Fundam. Crystallogr.*, 1990, **A46**, 467.
50 R. J. Cernik, W. Clegg, C. R. A. Catlow, G. Bushnell-Wye, J. V. Flaherty, G. N. Greaves, M. Hamichi, I. Burrows, D. J. Taylor and S. J. Teat, *J. Synchrotron Radiat.*, 1997, **4**, 279.